Biophysical Chemistry 182 (2013) 58–63

Contents lists available at ScienceDirect

Biophysical Chemistry

journal homepage: http://www.elsevier.com/locate/biophyschem

Raman micro-spectroscopy: A powerful tool for the monitoring of dynamic supramolecular changes in living cells

Silvia Caponi [a,b,*], Lavinia Liguori [c], Alessandra Giugliarelli [d], Maurizio Mattarelli [e], Assunta Morresi [d], Paola Sassi [d], Lorena Urbanelli [f], Carlo Musio [a]

[a] Istituto di Biofisica, Consiglio Nazionale delle Ricerche, c/o Fondazione Bruno Kessler, Via alla Cascata 56/C, 38123 Trento, Italy
[b] Dipartimento di Fisica, Università di Trento, Via Sommarive 14, 38050 Povo, Trento, Italy
[c] Equipe SyNaBi, Laboratoire TIMC UMR CNRS 5525, Université J Fourier, Domaine de la merci, 38700 La Tronche, France
[d] Dipartimento di Chimica, Università di Perugia, Via A. Pascoli, I-06100 Perugia, Italy
[e] NiPS Laboratory, Dipartimento di Fisica, Università di Perugia, Via A. Pascoli, I-06100 Perugia, Italy
[f] Dipartimento di Medicina Sperimentale e Scienze Biochimiche, Università di Perugia, Via del Giochetto, I-06123 Perugia, Italy

HIGHLIGHTS

- The cellular death is investigated by Raman micro-spectroscopy in T-lymphocytes.
- Insights to underlying cellular activities have been found.
- Markers in the membrane modifications induced by cellular death are indicated.

GRAPHICAL ABSTRACT

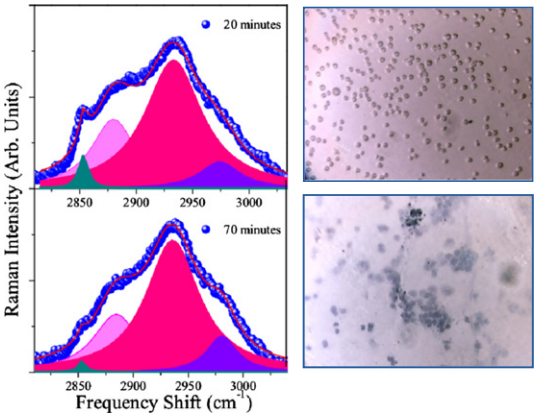

ARTICLE INFO

Article history:
Received 7 May 2013
Received in revised form 18 June 2013
Accepted 18 June 2013
Available online 27 June 2013

Keywords:
Raman spectroscopy
Cellular death
Cellular imaging
Apoptosis process
Necrosis process
Jurkat cell

ABSTRACT

Cellular imaging techniques have become powerful tools in cell biology. With respect to others, the techniques based on vibrational spectroscopy present a clear advantage: the molecular composition and the modification of subcellular compartments can be obtained in label-free conditions. In fact, from the evolution of positions, intensities and line widths of Raman and infrared bands in the cell spectra, characteristic information on cellular activities can be achieved, and particularly, cellular death can be investigated. In this work we present the time evolution of the Raman spectra of single live Jurkat cells (T-lymphocyte) by looking at the high frequency part of their Raman spectra, that is the CH stretching region, around 3000 cm^{-1}. In particular, investigation into the composition or rearrangement of CH bounds, markers of cellular membrane fatty acids, can represent an important method to study and to recognize cell death. The experimental procedure we used, together with the analysis of these high frequency vibrational bands, may represent a new, improved and advantageous approach to this kind of study.

* Corresponding author at: Istituto di Biofisica, Consiglio Nazionale delle Ricerche, c/o Fondazione Bruno Kessler, Via alla Cascata 56/C, 38123 Trento, Italy. Tel.: +39 0461 314 628.
E-mail address: silvia.caponi@cnr.it (S. Caponi).

0301-4622/$ – see front matter
http://dx.doi.org/10.1016/j.bpc.2013.06.013

1. Introduction

Among all the available physico-chemical approaches, spectroscopic investigations are more and more successfully applied to complex systems of biological interest. In particular, vibrational FTIR and Raman spectroscopies are label-free, non invasive methods, very useful for the study of cellular systems without staining them. Following the changes of IR and Raman band-shapes in cooling–thawing cycles, information can be obtained about cell behaviour, membrane phase transitions and modification of membrane properties, together with water–ice transitions [1–4]. The coupling of optical microscopy devices to the usual Raman spectroscopic set-up is particularly effective when used to investigate animal and human cellular samples, characterizing different macromolecules inside single living cells and providing optical markers for cytological analysis [5–8].

Cellular death is widely investigated in biomedicine, in order to understand the different mechanisms underlying the biochemical modifications taking place during cellular and tissue consumption in biological samples.

Considering that de-regulation or alteration of cell death processes are the key events in a wide range of human diseases and despite the different mechanisms engaged by nature to lead cellular death, direct monitoring of cells during those processes is desirable to determine their molecular outcome.

One can collect a great number of possible origins of cellular death, referring to the two principal paths, that is necrosis and apoptosis. The differences are well known: necrosis is a death induced by a traumatic external treatment usually associated with inflammation, a sort of "cellular murder", while apoptosis is a programmed cell death process, a sort of "cellular suicide" involved in physiological tissue development. The first can be caused by physical agents, such as temperature stress and ionizing radiation, or can be chemically (by drugs, for example), or biologically (viral agents) induced, while the second one depends on the intrinsic nature of the cells, although it could be also initiated by extracellular processes. Usually apoptosis regards single cells, while necrosis affects groups of neighbouring cells [9]. The two processes can be observed and distinguished in the same cellular samples: the efficacy of cancer therapies, for example, can be evaluated by an estimation of tumour necrosis [10], but at the same time apoptosis can be initiated by chemiotherapeutic agents [11].

It is thus crucial to be able to identify and characterize putative markers for cell death in the case of necrosis and/or apoptosis: different cellular components are in fact involved in the two death processes. Apoptosis usually involves sequential condensation and fragmentation of nuclear DNA that can be followed by treating cells with dyes that link to nucleic acids (ex. Hoechst 33258), while necrotic cells are characterized by the rupture of the cellular membrane, usually visualized by Trypan blue assay.

The tests on living cells have some important limits: first of all, it is not possible to use the same biological sample after the test; second, they need target molecules to be labelled to give information about the involved molecular mechanisms. During cryopreservation to build cell banking used in cell-based therapies of particular cells and tissues, the so called cryoinjury of single cells in the cooling–thawing cycles is the principal cause of cellular death (necrosis, in this case) that can prejudice the whole banking process and the efficacy of the final clinical use of the cells [12]. Even if the macroscopic effect of cooling–thawing is well known, the available information about the detailed processes inside the biological samples is insufficient for their comprehension at a molecular level. The optimization of the cooling–thawing procedure, together with the choice of the best cryoprotectants, depends on how deep the knowledge is on cell necrosis at a molecular level.

MicroRaman spectroscopy has been used in explorative measurements to study both apoptosis and necrosis processes, in different cellular samples [13–16]: The observed modifications of the recorded spectra have been associated with biochemical changes in cell samples, without any definitive conclusions about the details of the mechanism, due to the scarcity of the systematic dedicated series of measurements even if the spectra are manipulated by fitting procedures and statistical treatments [17].

Up to now, the available vibrational spectra, IR and Raman ones, usually regard the region under 1800 cm^{-1}, where it is possible to individuate nucleic-acid backbones, DNA, RNA, proteins and lipid vibrations. About IR spectra, the high intensity of OH stretching vibrations interferes with the lower intense CH_2 peaks that cannot be easily recorded in absorption experiments. As the first attempt to overcome the above poverty of indications, the present paper reports microRaman measurements of T-lymphocites at different hydration conditions and as a function of time, that allow individuating the modifications associated to cellular membrane through the spectral modifications in the CH stretching region.

The band shape analysis of Raman spectra that we propose, collected with a particular experimental procedure, suggests the choosing of the CH_2 stretching signals as band markers, in order to follow efficaciously the biochemical modifications associated the membrane status linked to the death process.

2. Materials and methods

2.1. Cell culture

Jurkat cells are a T-lymphocyte immortalized human cell line used to study T-cell leukaemia, chemokine expression receptors susceptible to viral entry and T-cell signaling [18]. They have been proven as a suitable model not only for the study of the T-cell receptor machinery but also for apoptosis [19]. In fact, several well-defined physiological, pharmacological, and pathological triggers are able to induce apoptotic effects on Jurkat cells.

Jurkat are non-adherent cells and cell culture was maintained in DMEM (Dulbecco's modified eagle medium) supplemented with 10% (v/v) heat-inactivated foetal calf serum, 100 U/ml penicillin and 100 U/ml streptomycin at 37 °C under 5% CO_2 and 95% air. Prior to use in experiments, 6 ml at 2×10^6 cells/ml was pelleted and prepared by 2 sequential centrifugations at 800 ×*g*, 5 min, the first one to remove the medium and the second one in 5 ml of PBS (Phosphate Buffered Saline buffer) to wash the cells and eliminate any residual medium contamination. After an addition of 20 μl of PBS the resultant pellet of cells was transferred in an eppendorf tube ready for Raman analysis.

2.2. Raman experiments and data treatment

The Raman spectra are obtained using a micro-Raman setup (Horiba Jobin-Yvon, model LabRam Aramis), equipped with a He–Ne laser of $\lambda = 632.8$ nm with a 10 mW power, an edge filter with O.D. higher than 8 which prevents the acquisition of Raman signal below 100 cm^{-1} from the laser line, a 1200 grooves/mm grating for a resolution of about 2 cm^{-1} as measured by fitting the Rayleigh line, and a Peltier cooled CCD detector (1024 × 256 Pixels) which, in the present conditions, allows the simultaneous acquisition of about 700 cm^{-1}. The experimental apparatus is equipped with different objectives: 10× and 50× plan apochromat air objectives and a water immersion UPLSAPO 60XW from Olympus. In the first used configuration, the used exciting source was focused onto the sample through a 50× objective with a 100 μm working distance. In this case the pellet was deposited onto a metallic slide under the microscope-objective. Evaporation leads to a low hydration level, and subsequent cellular death in a few minutes of waiting time. To reduce the evaporation a second configuration was adopted: the pellet of cells in suspension was deposited onto a metallic slide and it was covered by a coverslip glass in order to maintain a high hydration level. In this case a water immersion objective is used. In fact thanks to its high numerical apertures, N.A. = 1.2, a working distance of 280 μm and its correction collar which allows adjustment to accommodate cover glass

thickness (an essential feature to eliminate spherical aberration in imaging experiments and to avoid the acquisition of glassy signals in the Raman spectra) the water immersion objective affords to reach high quality images and spectra. Moreover, the chosen objective exhibits high transmission and chromatic aberration correction from the near ultraviolet to the red visible spectral regions, making its performance useful for the Raman imaging of living cells in a wide frequency range.

A Trypan blue viability test showed that the glass coverslip preserves cell life for more than 1 h.

Raman spectra were collected in the 100–4000 cm^{-1} range. The frequency calibration was performed using the spectral lines of an Argon lamp. The total spectra were obtained by recombining several spectral regions acquired successively by the CCD. The acquisition time per pixel ranged from 100 to 600 s. The spectra were corrected by the instrumental response function obtained by a black body emission measurement, in order to remove the frequency dependence of the grating, CCD and filter responsivity. Once corrected for the instrumental response function, the Raman spectra present a broad luminescence background, which depends on the exposition time to the laser light, on the different focalization conditions and on the samples conditions. Different methods were developed to effectively subtract the luminescence background [20]. In our case, while not affecting the observation of the evolution of the much sharper molecular peaks, the luminescence was subtracted, by fitting it with a 5th degree polynomial in order to ease the comparison of different spectra. As an exemplum, the typical Raman spectrum from a dry Jurkat cell and its estimated luminescence background is reported in Fig. 1.

The spatial resolution of the microRaman spectrometer is around 2 μm and allows the obtaining of spectra on a single cell or on different positions inside the same cell, due to the fact that with a low hydration condition the cell is not able to move.

3. Results and discussion

Fig. 2 shows the image of the cell pellet deposited on a metallic substrate acquired by the 50× air objective in a very low hydration condition.

The objective of the microscope was the same when used to visualize in a camera the cell images and also to acquire the scattered inelastic signal once the sample was illuminated by the laser. The typical Raman spectrum for a single Jurkat cell is presented in Fig. 3a for a wide frequency range. The acquisition time is 100 s per pixel and the total time required for this spectrum is 500 s. The observed vibrations have already been described in literature [21,22]. The lower frequency zone of the spectrum, dominated by the vibration bands of the nucleic acids and proteins, is reported magnified in Fig. 3b, while in Fig. 3c the bands related to the CH vibrational modes are evidenced. In particular, the main broad peak centred at about 2932 cm^{-1} and its high-frequency shoulder are assigned to vibrations of lipids and proteins while the sharper peaks (at about 2854 and 2874 cm^{-1}) which appear on the low frequency wing of the profile are related to the vibrational modes of the membrane lipids [23,24]. The used experimental conditions, due to the fast acquisition time and the laser characteristics, ensure the absence of photo-bleaching or chemical reactions initiated by the laser power in the cell.

It is noteworthy that due to the measurement conditions, the spectrum is relatively free from the water signal (whose main contribution is the weak broad band centred at about 3300 cm^{-1}) as well as from the substrate contributions. In addition, the low hydration conditions allow us to collect spectra of different compartments of a single cell stuck on the substrate. However, even if highly packed cells keep longer water content, the cells viability is strongly affected and reduced to about 10–15 min due to inevitable evaporation.

To study the Raman spectra associated with cell ageing in a hydrated condition a further analysis has been performed using the second

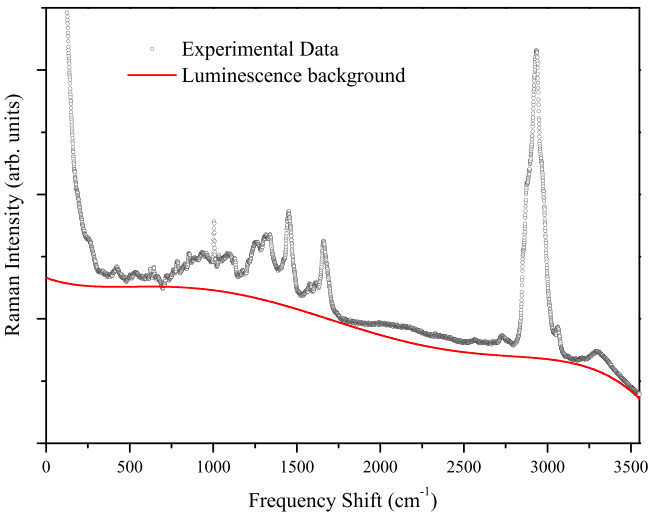

Fig. 1. Raman Spectrum (open circles) and its estimated luminescence background (line).

experimental design with the use of the cover glass and water immersion objectives. In this case it is possible to follow the dynamic supramolecular changes in living cells and in particular during cellular death. By a Trypan blue viability test and by the evolution in the shape of the cells, the estimated death time is around 1 h. The image of the fresh pellet suspension, obtained by centrifugation and successive wash of the cells in PBS is reported in Fig. 4. For the highly concentrated suspension of cells in PBS, we analyse the complete vibrational spectrum as a function of time. The complete spectrum of the fresh pellet once the luminescence contribution has been subtracted, is reported as open circles in Fig. 5, where for comparison the buffer solution spectrum is also shown as a full line. The two spectra were normalized to the O–H stretching band of water which dominates the spectra of the analysed samples from 3000 to 3600 cm^{-1}. Another less intense solvent contribution is related the H–O–H bending mode: it is centred at around ~1640 cm^{-1}, superimposed to the spectral feature of the fatty acids and the amide I vibrational modes [10]. In the remaining spectral regions the PBS contribution is a flat background on which the characteristic features of the cell vibrational modes stand out. In the inset of Fig. 5 the zoom of the band related to the CH_2 and CH_3 stretching vibrational modes is reported. In the present work we concentrate our attention on the evolution of this particular band during cell death, considering this analysis as a key to access the cell membrane state.

The time evolution of the band centred at about 2900 cm^{-1} is reported in Fig. 6. In particular in Fig. 6a and Fig. 6b the measured spectra of the cell suspension and the relative PBS contribution normalized to the H–O–H bending mode is reported for two different waiting times from the pellet formation: $t_w = 20$ min and $t_w = 70$ min. Just from the raw data, a clear change of this band shape is observed: the peaks (at ~2850 cm^{-1} and ~2875 cm^{-1}) assigned to the CH_3 and CH_2 symmetric and asymmetric stretching of lipids [24], which in the Jurkat cells are concentrated in the membrane, become scarcely visible in the 6b spectrum.

A more accurate comparison can be achieved from Fig. 6c, where the spectra, once the water contribution is subtracted, are reported for different waiting times ($t_w = 20, 40, 70$ min) in the dry samples. For comparison the spectra are normalized on the peak centred at ~2935 cm^{-1}. These buffer free spectra present a clear trend in their modification. Even if both peaks related to the lipids vibrational modes reduce their intensity, the relative change is different. As obtained from the band shape analysis reported in Fig. 7, the intensity of the 2850 cm^{-1} peak is reduced by about 70%, while in the peak centred at ~2875 cm^{-1} the reduction is about 15%. It is worth noticing that the spectrum of the dry sample is practically coincident with that acquired after the

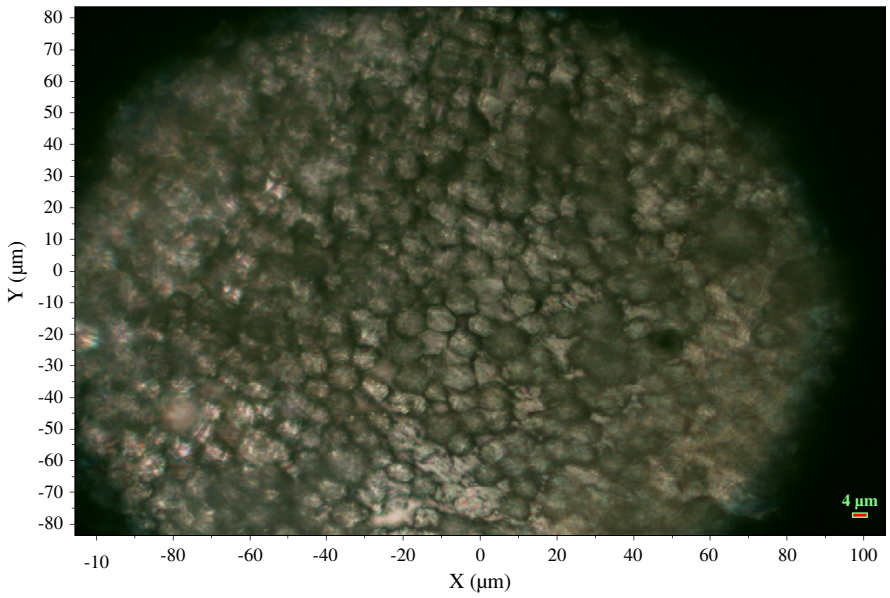

Fig. 2. Images of Jurkat cells investigated by Raman Spectroscopy. Fresh pellet in a very low hydration condition magnificated with a 50× Olympus objective.

cell death in the hydrated condition, having subtracted the water contribution.

The band shape analysis was performed by a fitting procedure with a Lorentzian shape including only the major four vibrations assigned for this frequency region [21]. Even if the presence of minor contributions in that frequency range is expected, we chose to include only the principal contributions in order to reduce as much as possible the fitting parameters. The good agreement between the experimental data and the band shape convolution assures the goodness of the adopted procedure. The width and the intensity of the peak centred at ~2932 cm^{-1} remain almost constant; on the contrary a clear intensity reduction is evident in the lower frequency contributions, while only a width variation is present in the peak at the highest frequency.

We would underline that a huge amount of studies were performed to characterize the evolution of this band in a large class of materials, which present polymethylene chains, ranging from SDS micelles [25,26], to cholesteric liquid crystals [27] and biomembranes [28,29]. It has been found that the ratio of the peak heights is sensitive to the structure of the chain environment (lateral packing) and to the conformational disorder [30]; the relative decrease of peak centred at 2850 cm^{-1} is a mark of the reduced ordering.

The observed spectral changes can be well explained in this framework.

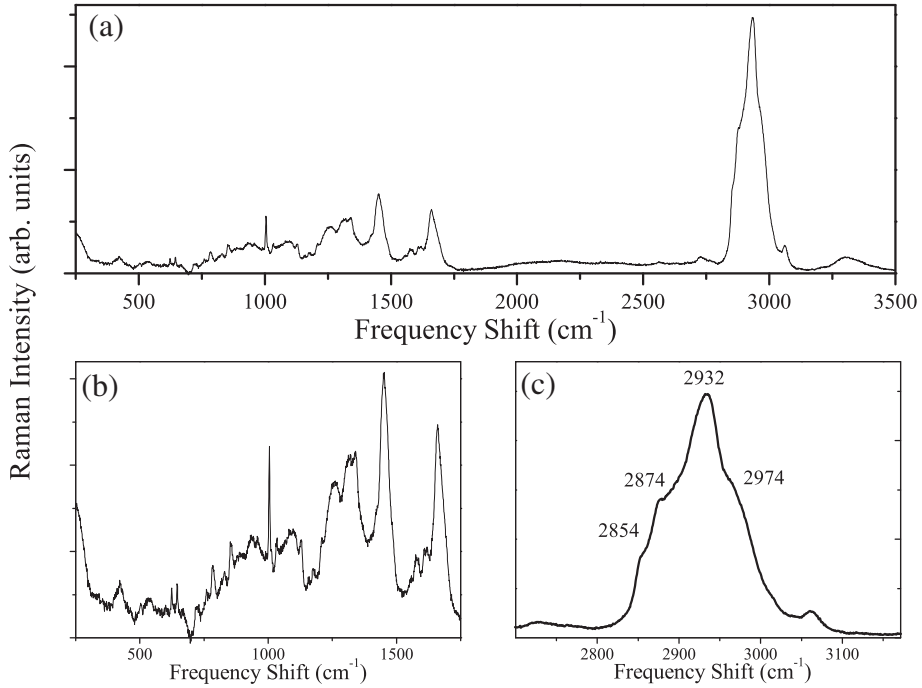

Fig. 3. a) Raman spectra in wide frequency range in a pellet at very low hydration condition (using a 50× Olympus objective). The frame b) and c) report the zoom in the two characteristic vibrational ranges of low and high frequency range respectively. The acquisition time is 100 s per pixel. The total time needed for acquiring this spectrum is 500 s.

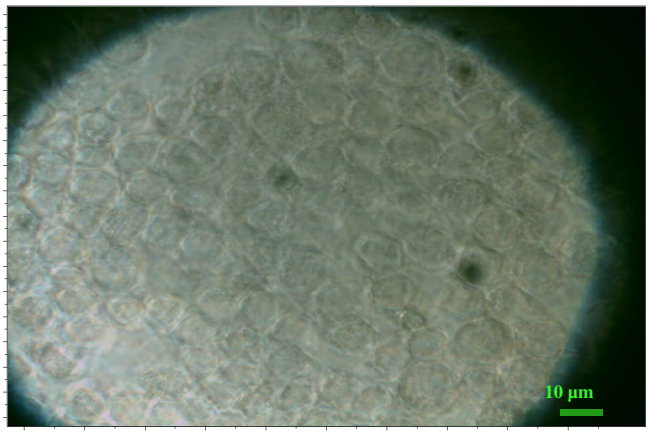

Fig. 4. Image of Jurkat cells investigated by Raman spectroscopy. Fresh pellet in high hydration condition magnificated with a 60× Olympus objective.

After cell death, it is well assessed that the cell membrane undergoes disruptive processes of the lipid organization named phospholipid scrambling [31], permeability alterations and blebbing phenomena caused by a decoupling of the cytoskeleton from the plasma membrane [32] These mechanisms lead to an increased disorder of the chain environment which is precisely caught by the evolution of the CH_2 and CH_3 stretching modes recorded in the Raman spectra.

Moreover, the reduced intensity of the low frequency side of the CH stretching profile respect to the higher one suggests that the relative amount of lipids with respect to proteins decreases in the dead cell. Actually, the sensitivity of Raman microspectroscopy to detect differences in the biochemical composition of cells has been recently evidenced [23]. In particular, Short and co-workers observed an increase in lipid amount due to the proliferation of mammalian cell cultures, thus, the maximum intensity of 2850–2880 cm^{-1} in the components we observed in the fresh sample, is qualitatively in agreement with these data and indicates that, not only a breakage but also a chemical degradation is suffered by the membrane during the cell death. The two recorded peaks could be considered efficacious and promising markers specifically for cell death. A further confirmation of our results is given by the spectroscopic analysis of methylene/methyl groups performed on doxorubicin-treated Jurkat T-cells [33]. The study, carried out by proton nuclear magnetic resonance spectroscopy (1H NMR), finds a strict correlation and a direct temporal relationship between the increase of the ratio CH_2/CH_3 signals intensities and apoptotic phenomena in

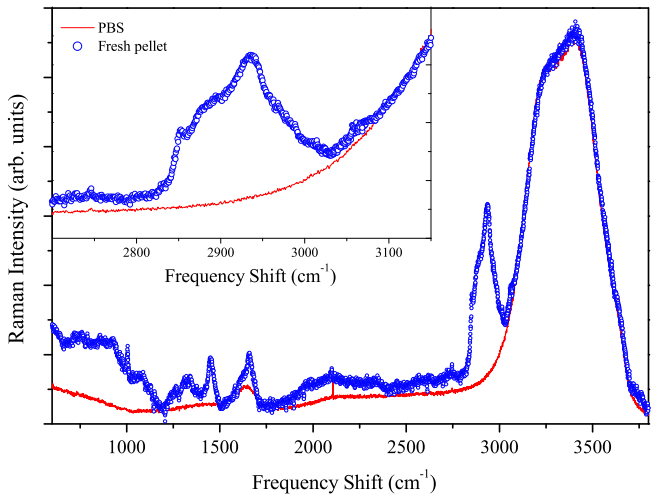

Fig. 5. Typical Raman spectra of the hydrated sample (Blue circles). The red line is the PBS spectrum. The data are normalized to the contribution at 3200 cm^{-1} associated to the OH vibrational modes. In the inset the zoom of the CH vibrational modes is reported.

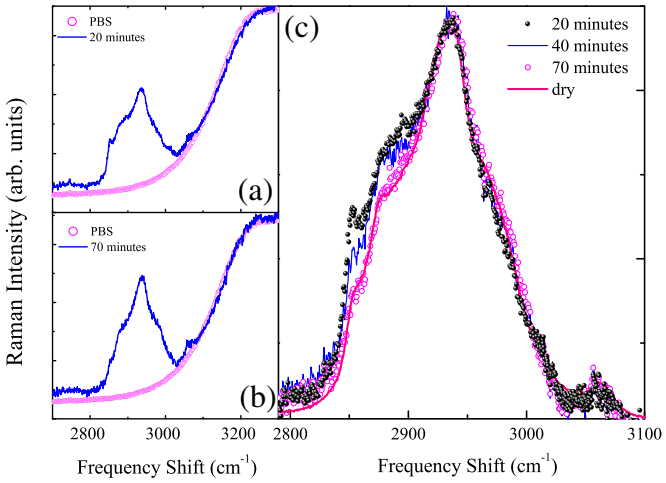

Fig. 6. a) and b) show the spectrum of the cells (blue line) and the PBS (red circles) respectively at t = 20 min and t = 70 min. c) Time evolution of the bands referred to CH vibrational stretching modes at different times after the subtraction of the buffer contribution.

lymphoblasts of patients suffering lymphoblastic leukaemia (ALL). The value of the CH stretching region as a putative bio-marker of apoptotic modifications at the cell membrane level has been confirmed.

In this sense, our future experimental work will be focused on understanding the behaviour of these two markers in apoptotic cells. We will induce apoptosis on different cell lines by using well described drugs active on different intracellular pathways and repeat the same procedure in order to define the contribution on the two peaks of interest. This study will allow us to generalize and to propose a so called "Raman death checking method".

4. Conclusions

For cell viability tests, a standard Trypan blue dye method relies on the alteration in membrane integrity as determined by the uptake of dye by dead cells. With our experimental procedure, we found that

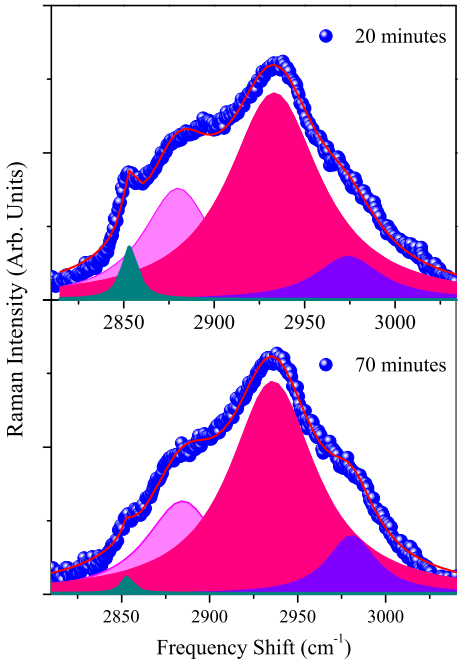

Fig. 7. Time evolution of Raman band centered at 2930 cm^{-1} acquired at two different waiting times, 20 min (upper panel) and 70 min (lower panel). The band shape analysis evidences the relative variation of intensity between the different contributions.

Raman spectroscopy can integrate in a label free condition the results from other techniques. While not being presently resolutive, our proposed approach promises to be a successful methodology for the elucidation of the cell state and the individuation of the effective death process by monitoring the alteration of membranes accessible by investigation of the vibrational properties of the CH stretching mode of membrane lipids. The identifications of spectral "markers" will represent the label-free supermolecular hallmarks of the death process, that can be used, e.g., for drug screening and cancer research. We are aiming, in future investigations, to demonstrate our approach as a novel and effective method holding promise for the discrimination between apoptotic and necrosis processes which occur in the cell life-span.

Acknowledgements

CNR Flagship Project "Nanomax (N-CHEM)" and PAT (Autonomous Province of Trento) "Grandi Progetti 2012" Project "MaDEleNA" partially granted this research. The work was done in collaboration and with the support of the Italian National Transplant Centre (CNT), Florence (Italy), within the Project "Cryopreservation of cell for human clinical use, with particular regard to certain types as mesenchymal, hematopoietic stem cells, and reproductive cells". LL was given a grant by the Bruno Kessler Foundation (FBK), Trento, Italy.

References

[1] K. Gousset, W.F. Wolkers, N.M. Tsvetkova, A.E. Oliver, C.L. Field, N.J. Walker, J.H. Crowe, F. Tablin, Evidence for a physiological role for membrane rafts in human platelets, J. Cell. Physiol. 190 (2002) 117–128.
[2] W.F. Wolkers, S.K. Balasubramanian, E.L. Ongstad, H.C. Zec, J.C. Bischof, Effects of freezing on membranes and proteins in LNCaP prostate tumor cells, Biochim. Biophys. Acta Biomembr. 1768 (2007) 728–773.
[3] D. Ami, T. Neri, A. Natalello, P. Mereghetti, S.M. Doglia, M. Zanoni, M. Zuccotti, S. Garagna, C.A. Redi, Embryonic stem cell differentiation studied by FT-IR spectroscopy, Biochim. Biophys. Acta 1783 (2008) 98–106.
[4] C.W. Freudiger, W. Min, B.G. Saar, S. Lu, G.R. Holtom, C. He, J.C. Tsai, J.X. Kang, X.S. Xie, Label-free biomedical imaging with high sensitivity by stimulated Raman scattering microscopy, Science 322 (2008) 1857–1861.
[5] G.J. Puppels, F.F. de Mul, C. Otto, J. Greve, M. Robert-Nicoud, D.J. Arndt-Jovin, T.M. Jovin, Studying single living cells and chromosomes by confocal Raman microspectroscopy, Nature 347 (1990) 301–303.
[6] E.B. Hanlon, R. Manoharan, T.W. Koo, K.E. Shafer, J.T. Motz, M. Fitzmaurice, J.R. Kramer, I. Itzkan, R.R. Dasari, M.S. Feld, Prospects for in vivo Raman spectroscopy, Phys. Med. Biol. 45 (2000) R1–R59.
[7] J. Chan, S. Fore, S. Wachsman-Hogiu, T. Huser, Raman spectroscopy and microscopy of individual cells and cellular components, Laser Photonics Rev. 2 (2008) 325–349.
[8] C. Krafft, B. Dietzek, J. Popp, Raman and CARS microspectroscopy of cells and tissues, Anal. (Lond.) 134 (2009) 1046–1057.
[9] A.I. Zhmakin, Fundamentals of Cryobiology, Springler, Berlin, 2009.
[10] W.S. Ahn, S.M. Bae, S.W. Huh, J.M. Lee, S.E. Namkoong, S.J. Han, C.K. Kim, J.K. Kim, Y.W. Kim, Necrosis-like death with plasma membrane damage against cervical cancer cells by photodynamic therapy, Int. J. Gynecol. Cancer 14 (2004) 475–482.
[11] A.E. Milner, D.H. Palmer, E.A. Hodgkin, A.G. Eliopoulos, P.G. Knox, C.J. Poole, D.J. Kerr, L.S. Young, Induction of apoptosis by chemotherapeutic drugs: the role of FADD in activation of caspase-8 and synergy with death receptor ligands in ovarian carcinoma cells, Cell Death Differ. 9 (2002) 287–300.
[12] M.J. Taylor, Y.C. Song, K.G.M. Brockbank, Life in the Frozen State, in: B.J. Fuller, N. Lane, E.E. Benson (Eds.), CRC Press, Boca Raton, 2004, pp. 603–641.
[13] N. Uzunbajakava, A. Lenferink, Y. Kraan, E. Volokhina, G. Vrensen, J. Greve, C. Otto, Nonresonant confocal raman imaging of DNA and protein distribution in apoptotic cells, Biophys. J. 84 (2003) 3968–3981.
[14] S. Verrier, I. Notingher, J.M. Polak, L.L. Hench, In situ monitoring of cell death using Raman microspectroscopy, Biopolymers 74 (2004) 157–162.
[15] N. Kunapareddy, J.P. Freyer, J.R. Mourant, Raman spectroscopic characterization of necrotic cell death, J. Biomed. Opt. 13 (2008) 054002.
[16] A. Zoladek, F.C. Pascut, P. Patel, I. Notingher, Non-invasive time-course imaging of apoptotic cells by confocal Raman micro-spectroscopy, J. Raman Spectrosc. 42 (2011) 251–258.
[17] Y.H. Ong, M. Lim, Q. Liu, Comparison of principal component analysis and biochemical component analysis in Raman spectroscopy for the discrimination of apoptosis and necrosis in K562 leukemia cells, Opt. Express 20 (2012) 22158–22171.
[18] R.T. Abraham, A. Weiss, Jurkat T cells and development of the T-cell receptor signalling paradigm, Nat. Rev. Immunol. 4 (2004) 301–308.
[19] C. Valavanis, Y. Hu, Y. Yang, B.A. Osborne, S. Chouaib, L. Greene, J.D. Ashwell, L.M. Schwartz, Model cell lines for the study of apoptosis in vitro, Methods Cell Biol. 66 (2001) 417–436.
[20] J.T. Motz, S.J. Gandhi, O.R. Scepanovic, A.S. Haka, J.R. Kramer, R.R. Dasari, M.S. Feld, Real-time Raman system for in vivo disease diagnosis, J. Biomed. Opt. 10 (2005) 031113.
[21] H.-J. van Manen, Y.M. Kraan, D. Roos, C. Otto, Single-cell Raman and fluorescence microscopy reveal the association of lipid bodies with phagosomes in leukocytes, PNAS 102 (2005) 10159–10164.
[22] V.V. Pully, A.T.M. Lenferink, C. Otto, Time-lapse Raman imaging of single live lymphocytes, J. Raman Spectrosc. 42 (2011) 167–173.
[23] C. Krafft, T. Knetschke, A. Siegner, R.H.W. Funk, R. Salzer, Mapping of single cells by near infrared Raman microspectroscopy, Vib. Spectrosc. 32 (2003) 75–83.
[24] K.W. Short, S. Carpenter, J.P. Freyer, J.R. Mourat, Raman spectroscopy detects biochemical changes due to proliferation in mammalian cell coltures, Biophys. J. 88 (2005) 4274–4288.
[25] M. Picquart, Vibrational mode behavior of SDS aqueous solutions studied by Raman scattering, J. Phys. Chem. 90 (1986) 243–254.
[26] G. Cazzolli, S. Caponi, A. Defant, C.M.C. Gambi, S. Marchetti, M. Mattarelli, M. Montagna, B. Rossi, F. Rossi, G. Viliani, Aggregation processes in micellar solutions: a Raman study, J. Raman Spectrosc. 43 (2012) 1877–1883.
[27] B.J. Bulkin, K. Krishnan, Vibrational spectra of liquid crystals. III. Raman spectra of crystal, cholesteric, and isotropic cholesterol esters, 2800–3100-cm^{-1} region, J. Am. Chem. Soc. 93 (1971) 5998–6004.
[28] B.J. Bulkin, N. Krishnamachari, Vibrational spectra of liquid crystals. IV. Infrared and raman spectra of phospholipid-water mixtures, J. Am. Chem. Soc. 94 (1972) 1109–1112.
[29] K.G. Brown, W.L. Peticolos, E. Brown, Raman studies of conformational changes in model membrane systems, Biochem. Biophys. Res. Commun. 54 (1973) 358–364.
[30] K. Larsson, R.P. Rand, Detection of changes in the environment of hydrocarbon chains by raman spectroscopy and its application to lipid–protein systems, Biochim. Biophys. Acta — Lipids and Lipid Metab. 326 (1973) 245–255.
[31] E. Lang, S.M. Qadri, F. Lang, Killing me softly — suicidal erythrocyte death, Int. J. Biochem. Cell Biol. 44 (2012) 1236–1243.
[32] O.T. Fackler, R. Grosse, Cell motility through plasma membrane blebbing, J. Cell Biol. 181 (2008) 879–884.
[33] F.G. Blankenberg, P.D. Katsikis, R.W. Storrs, C. Beaulieu, D. Spielman, J.Y. Chen, L. Naumovski, J.F. Tait, Quantitative analysis of apoptotic cell death using proton nuclear magnetic resonance spectroscopy, Blood 89 (1997) 3778–3786.